Rheol Acta (2010) 49:979–984
DOI 10.1007/s00397-010-0456-7

RAPID COMMUNICATION

Evaluation of drag correction factor for spheres settling in associative polymers

Arturo J. Mendoza-Fuentes · Octavio Manero · Roberto Zenit

Received: 6 November 2009 / Revised: 16 April 2010 / Accepted: 22 April 2010 / Published online: 16 May 2010

Abstract Drag correction factors are calculated for the creeping motion of spheres descending in various associative polymers of different concentration with various sphere-container ratios and Weissenberg numbers. The simple-shear rheology and linear viscoelasticity of these polymeric fluids have been previously presented and modeled with the BMP (Bautista–Manero–Puig) equation of state (Mendoza-Fuentes et al., Phys Fluids 21:033104, 2009). The drag on the sphere is initially kept nearly constant for small Weissenberg numbers, We $<$ 0.1. As the Weissenberg number increases, We $<$ 0.1, a reduction in drag is found. Experimental results show the presence of a critical Weissenberg number at which a drag reduction occurs. The reduction in the drag correction factor is associated to the onset of extension-thinning, which coincides with the formation of a negative wake. No increase in the drag correction factor was observed, due to the simultaneous opposing effects of extension-thickening and shear-thinning viscosity. The shape of the drag correction factor curve may be predicted considering the extensional properties of the solutions, as suggested elsewhere (Chen and Rothstein, J Non-Newton Fluid Mech 116:205–215, 2004).

A. J. Mendoza-Fuentes
Facultad de Química, Universidad Nacional Autónoma de México, México 04510, México

O. Manero · R. Zenit (✉)
Instituto de Investigaciones en Materiales, Universidad Nacional Autónoma de México, Apdo. Postal 70-360, México 04510, México
e-mail: zenit@unam.mx

Keywords Drag correction factor · Flow around spheres · Associative polymers

Introduction

Many theoretical and experimental studies of the motion of a sphere falling in non-Newtonian fluids have been conducted. This subject may be considered one of the cornerstone problems in modern fluid dynamics. Its importance ranges from industrial problems, such as suspending heavy abrasive particles in mobile liquid detergents and particle transport by well-technology fluids in the oil industry (Chhabra 1993), to fundamental investigation to test constitutive models and numerical methods of non-viscometric flows (Walters and Tanner 2002).

Despite several decades of investigations, some issues have not been studied in detail or remain unsolved (Owens and Phillips 2002). For example, the influence of elasticity and shear-thinning behavior on the drag coefficient have not been completely elucidated. Within a historical perspective for the case of highly elastic constant viscosity fluids (the so-called Boger fluids) and for a small value of the sphere-container ratio, it has been shown that the drag correction factor, K (defined below), has no significant deviations from the Stokesian value at small Weissenberg numbers, We $<$ 0.1; the Weissenberg number is defined as

$$\mathrm{We} = \lambda U/a, \tag{1}$$

where λ is the relaxation time, U and a are the sphere velocity and radius, respectively. Instead of the Weissenberg number, some authors use the Deborah

number, De. However, their physical interpretation is not the same as discussed by Elmoumni and Winter (2006). To avoid any confusion, we only used the data of other authors who define the Weissenberg number as in Eq. 1.

For intermediate values of the Weissenberg number, $0.1 < \mathrm{We} < 1$, a reduction in the drag coefficient is observed, and for $\mathrm{We} > 1$, a nearly constant value of drag coefficient is reached; finally, the drag correction factor increases for large We numbers. In general, the shape of the drag correction factor for these fluids depends on the extensional properties of the fluid and geometric aspect ratios used (Jones et al. 1994). For the case of shear-thinning viscoelastic fluids, Sigli and Coutanceau (1977) found, for polyethylene oxide solutions, a reduction in the drag correction factor of nearly 60% less than the Stokes value once the first normal stress difference departs from the quadratic region, thus attributing this phenomena to fluid elasticity. The sphere-container ratios used by Sigli and Coutanceau (1977) were within $0.25 < a/R < 0.5$, where a is the sphere radius and R is that of the container.

Using a 1% aqueous polyacrylamide solution Bisgaard (1983) found, for an aspect ratio $a/R = 0.5$, a reduction in the drag correction factor; for lower aspect ratios, $a/R = 0.4$ and $a/R = 0.3$, a nearly constant value of the drag correction factor with We was found. Further studies by Mena et al. (1987) revealed that in the low shear rate region elastic effects were the predominant factor for drag reduction, but at higher shear rates, shear-thinning took over as the primary cause for further drag reduction. Navez and Walters (1996) confirmed results by Mena et al. for high aspect ratios where viscoelastic effects were smaller than shear-thinning effects, and later they were confirmed by Arigo and McKinley (1997) with small aspect ratios. In the above studies, a considerable reduction of the drag correction factor normalized by the Newtonian drag correction factor, K/K_N, is apparent; in the case of the polyacrylamide solution used by Navez and Walters an increase of this ratio was observed for $\mathrm{We} > 1$.

Additional experiments on the dependency of K on a/R were performed for high aspect ratios by Degand and Walters (1995). Values of the normalized drag correction factor, K/K_N, for a high aspect ratio, $a/R = 0.88$, showed a reduction of almost 85% of the drag correction factor with respect to the Stokes value.

More recently, Chen and Rothstein (2004) observed a decrease of drag correction factor with We for two aspect ratios in a wormlike micellar solution. In comparison to the drag correction factor curve for Boger fluids, their results show the presence of a second decreasing region at high We numbers. Their results show that for small Weissenberg numbers the drag correction factor is similar to that found in the Newtonian fluid. As We increases, K decreases due to shear-thinning effects. For $\mathrm{We} = 2$, the factor reaches a minimum. Increasing the Weissenberg number further, leads to an increase in the drag correction factor. This increase was attributed to a strong inhomogeneous extensional flow which develops in the wake of the sphere due to the large extension rates and resident times experienced by the wormlike micelles, leading to significant strain hardening and deformation of micelles. Additionally, Chen and Rothstein observed the presence of a critical We number where the flow becomes unstable, attributed to a breakdown of the wormlike micelle network structure in the wake of the sphere. Moreover, a third region where drag increased further at higher We numbers was also observed.

In summary, the general scheme of the behavior of the normalized drag correction factor with Weissenberg number found experimentally by different authors is depicted schematically in Fig. 1. Region A–D has been observed in Boger fluids; notwithstanding, shear-thinning viscoelastic fluids have shown the same behavior without the appearance of region C; furthermore, region E has been detected in wormlike fluids like those analyzed by Chen and Rothstein (2004).

Sedimentation of spheres in complex fluids and associated phenomena such as the behavior of drag correction factor are still unresolved problems that require further examination to be properly understood. In this work, we conduct an experimental study on the drag correction factor, using data of falling spheres in a

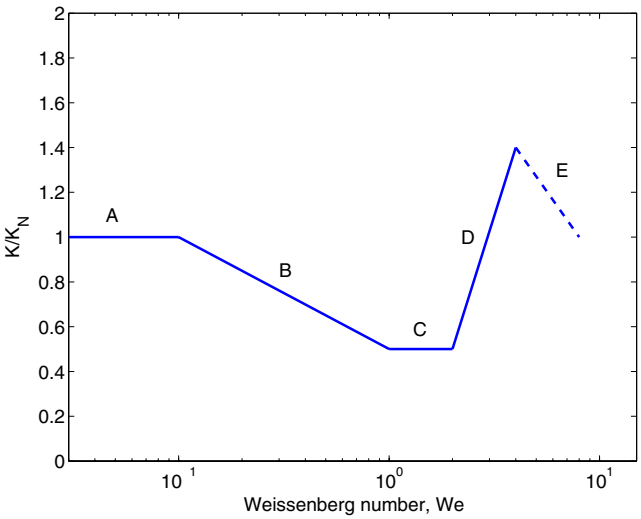

Fig. 1 General scheme of the behavior of the normalized drag correction factor with Weissenberg number

container filled with an associative polymer (hydrophobic alkali soluble emulsion, HASE) at various polymer concentrations in water. These polymers, namely associative polymers, form an elastic network joined by electrostatic interactions and physical entanglements, in the concentrated regime. The complexity of the flow behavior of falling spheres, in general and in particular, is manifested in interesting phenomena resulting from the viscoelastic, surface and time-dependent properties of the fluid (Puig et al. 2007). The study of these phenomena is the subject of the present investigation.

Experimental setup and conditions

The experimental arrangement comprises a cylindrical container of 120 cm length and 12.7 cm diameter ($R = 6.35$ cm); the container has a valve at the bottom to collect the spheres, which are released into the solution by a special mechanism to minimize surface and inertial effects. Four fluids were used corresponding to four polymer concentrations (1.0%, 1.5%, 2.0% and 2.5% of HASE by weight in water). The spheres tested have sizes (in centimeters) and densities (in kilograms per cubic meter) varying from 0.635 to 1.9 and 1.14 to 14.95, respectively. With these experimental conditions, the sphere to cylinder size ratio, a/R, ranged from 0.05 to 0.15.

To calculate the drag correction factor, five tests of each sphere-fluid combination were conducted to obtain a mean velocity with an uncertainty of about 0.1%. The flow visualization technique and fluid preparation procedures have been previously discussed elsewhere (Mendoza-Fuentes et al. 2009).

To account for the presence of walls and fluid viscoelasticity, we use the drag correction factor:

$$K = \frac{U_{\text{Stokes}}}{U_s} = \frac{2ga^2(\rho_s - \rho_f)}{9\eta_o U_s} \tag{2}$$

where g, a, η_o, U_s, ρ_s and ρ_f correspond to the gravity, sphere radius, zero shear viscosity, terminal velocity, sphere density and fluid density, respectively. For a Newtonian fluid, the drag correction factor takes the form:

$$K_N = \frac{1}{1 - f(a/R)} \tag{3}$$

where $f(a/R)$ is the Faxen's series:

$$f(a/R) = 2.1044(a/R) - 2.0877(a/R)^3 + 0.84913(a/R)^5 + 1.3720(a/R)^6 - 3.87(a/R)^8 + 4.19(a/R)^{10} \tag{4}$$

Thus, the ratio K/K_N, namely the normalized drag correction factor, is used to quantify the deviation from the Stokesian value due to the presence of walls and fluid viscoelasticity.

Modeling and fluids rheology

The modeling of fluid rheology has been described previously by Mendoza-Fuentes et al. (2009); only a brief discussion is presented here.

In Fig. 2 model predictions for uniaxial extensional flow and simple shear data are shown for the four HASE concentrations. A region of constant extensional viscosity at low extension rates ($\dot{\epsilon} < 10$) is followed by a strain-thickening region. The onset for the increasing viscosity coincides with that of shear-thinning, and the magnitude of the maximum in the extensional viscosity increases with concentration, although this increase is more pronounced in the dilute system. As in simple shear, the onset for strain thickening shifts to lower strain rates as concentration increases. This behavior has been associated to the evolution of intra-molecular junctions into intermolecular links as flow strength increases. The formation of an intermolecular network results in increasing elasticity and hence strain thickening. Because extensional flow deforms the system more drastically than simple shear, the extension thickening is normally more pronounced

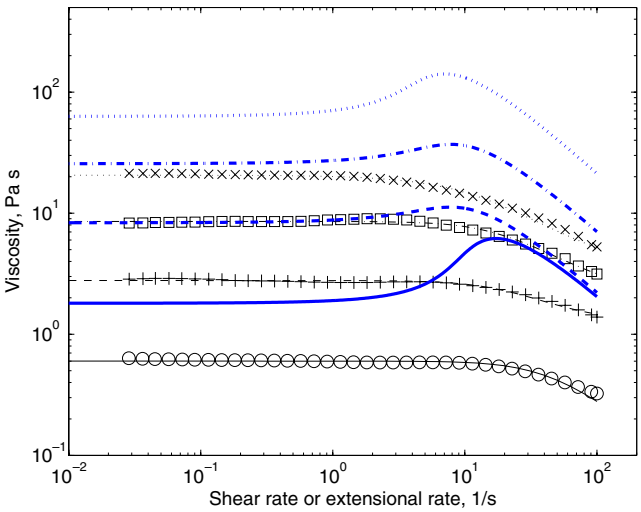

Fig. 2 Measured shear viscosity (symbols) and model predictions for shear and uni-axial extensional flows (*thin* and *thick lines*, respectively). (*Circles*) and (*solid line*), HASE 1.0%; (*plus symbol*) and (*dashed line*), HASE 1.5%; (*squares*) and (*dashed dotted line*), HASE 2.0%; (*multiplication symbol*) and (*dotted line*), HASE 2.5%

than shear thickening. At larger strain rates, the intermolecular associations break, leading to structure rupture and hence strain thinning. The predictions from the BMP model agree very well with the measurements in simple shear flow. For the case of extensional viscosity, the comparison between the predictions of the model and experimental measurements showed very good agreement (see Fig. 6 in Mendoza-Fuentes et al. 2009).

Results

The experimental value of the drag coefficient is obtained from measurements of the terminal velocity calculated from the displacement of the sphere in consecutive frames in the imaging system used by Mendoza-Fuentes et al. (2009). In Fig. 3, the normalized drag correction factor K/K_N is plotted as a function of We for different aspect ratios for the four liquids used in this investigation. In all fluids (HASE 1.0 to 2.5%) the drag correction factor remains constant around one for small We, and no substantial deviation from the Stokesian value is found. As We increases, a reduction of the drag correction factor is observed. The value of We where this drag reduction begins depends on fluid concentration and can be related to the appearance of the negative wake. We determined wether or not the negative wake had appeared in each case from the visualizations of Mendoza-Fuentes et al. (2009). In the figure, the data for which the negative wake was observed coincide with the cases in which drag reduction is present. This critical We may also be estimated by locating the onset for extension-thinning (see Fig. 9 in Mendoza-Fuentes et al. 2009). Note also that drag reduction has been observed for the case of bubbles ascending in HASE (Soto et al. 2007), which also coincides with the apparition of the negative wake.

In Fig. 4, a summary of all experimental results is depicted; the dependence of drag reduction on polymer concentration and We is clearly observed. A plateau region with no dependence on aspect ratio and fluid concentration is shown for We lower than 0.5. Past this value, the maximum drag reduction is near 40%; however, drag increase was not observed at all for large values of We. This is in agreement with the suggestion of Dou and Phan-Thien (2004), later confirmed by Mendoza-Fuentes et al. (2009), that less strain-thickening extension viscosities with a high value of extensional rate are the governing mechanisms for drag

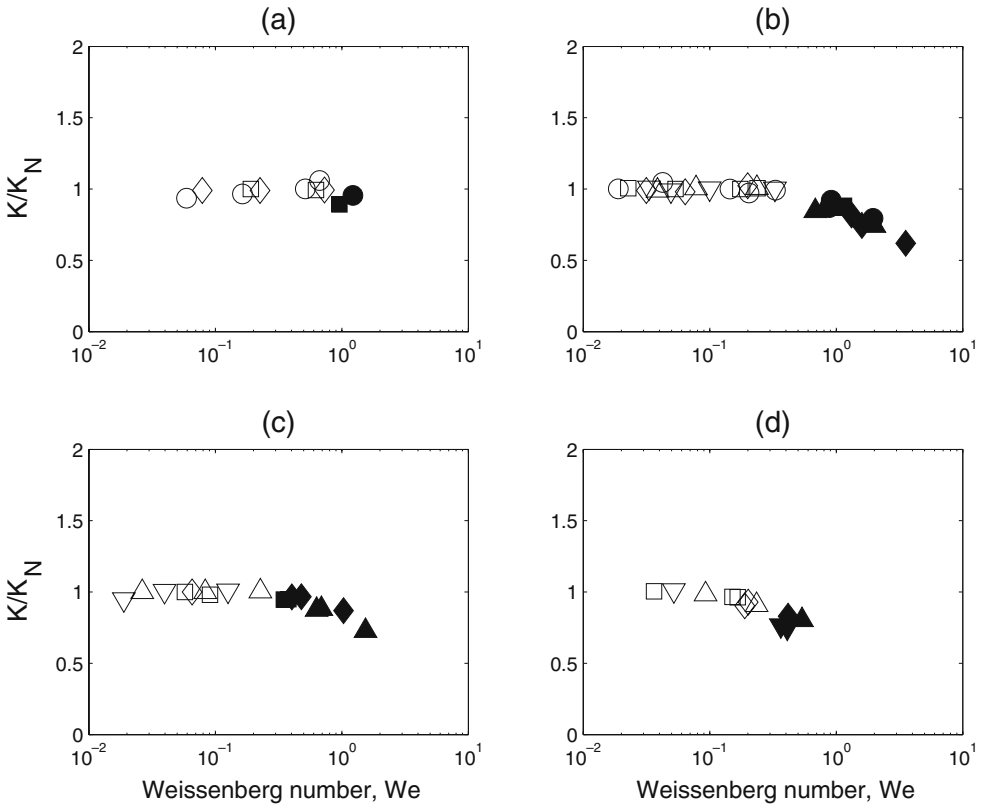

Fig. 3 Normalized drag correction factor, K/K_N, as a function of Weissenberg number, We, for all the liquids tested: **a** HASE 1.0%; **b** HASE 1.5%; **c** HASE 2.0%; **d** HASE 2.5%. Each symbol represents a different value of a/R: (*Empty circles*), a/R = 0.05; (*empty squares*), a/R = 0.0625; (*empty diamonds*), $a/R = 0.075$; (*empty triangles*), a/R = 0.1; (*inverted empty triangles*), a/R = 0.15. The filled and empty symbols represent the cases for which the negative wake had appeared or not, respectively, according Mendoza-Fuentes et al. (2009)

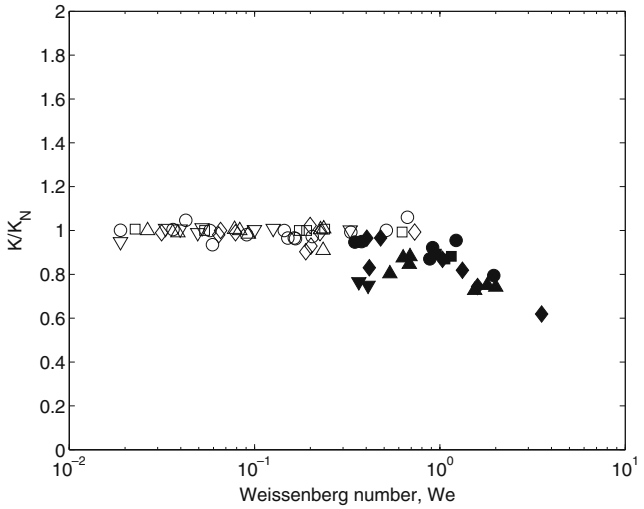

Fig. 4 Normalized drag correction factor, K/K_N, as a function of Weissenberg number, We, for all the liquids tested. All symbols are as in Fig. 3

reduction and negative wake appearance in the associative polymers examined here. However, in a wormlike micellar solution, Chen and Rothstein (2004) found a strong extensional flow with significant micelle deformation and strain hardening, which leads to the presence of a third region where a maximum in the drag correction factor occurs (region D, Fig. 1).

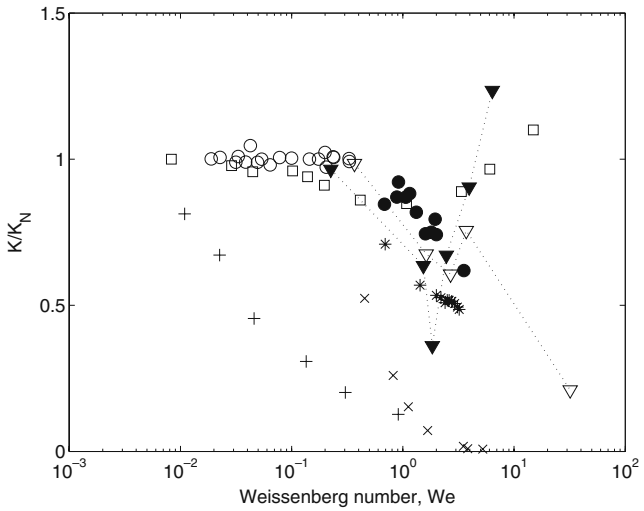

Fig. 5 Normalized drag correction factor, K/K_N, as a function of Weissenberg number, We, for the 1.5 wt.% fluid , shown as *filled* and *empty circles*. Experimental results from other authors: (*empty squares*), Navez and Walters (1996); (*plus symbol*), Degand and Walters (1995); (*asterisks*), Mena et al. (1987); (*multiplication symbol*), Arigo and McKinley (1997); (*inverted filled triangles*) and (*inverted empty triangles*), Chen and Rothstein (2004) (for this case, the *dotted lines* serve only as eye-guides)

In Fig. 5, a comparison of our experimental results using the 1.5 wt.% solution with data from other authors is shown. It is possible to observe the four main regions (marked as A, B, D and E) depicted in Fig. 1. The data published by Navez and Walters (1996) and Degand and Walters (1995) using the fluid S1 (solution of polyisobutylene in a solvent) show a quite different behavior. The fluid by Navez and Walters shows an increase in the drag correction factor for We $>$ 1, while the fluid by Degand and Walters only presents a drag reduction behavior. A possible explanation relays on the different extensional properties of the solvent used by these authors; while Navez and Walters used a mixture of polybutene oil and decalin, Degand and Walters used a solvent mixture of polybutene and 2-Chloropropane. In the same manner, the fluids used by Arigo and McKinley (1997) and by Mena et al. (1987) only present a drag reduction behavior with a maximum reduction of 50% and 63%, respectively, with increasing We. Notwithstanding, the data from Mena et al. show the presence of a nearly constant drag coefficient (region C in Fig. 1) for 1.5 $<$ We $<$ 3. Once more, the test fluids used by these authors were 2 and 8 wt. % polyacrylamide solutions in different solvents.

For the specific case of micellar fluids, similar to those used here, the only comparison that can be conducted is with the data of Chen and Rothstein (2004). in their case, a drag reduction is observed for We $<$ 2, in accordance with our results. however, for higher values of We for the two fluids that they considered, a strong drag increased (region D, Fig.1) is observed, followed by a second drag decrease behavior (region E, Fig. 1), but only for one of their test fluids. The appearance of regions D and E for We $>$ 4 was attributed to the presence of instabilities due to the scission of individual wormlike micelles and the breakdown of the entangled micelle structure. Hence, the coupled effect of shear-thinning and reduction of extensional viscosity may explain the behavior observed by Chen and Rothstein and that revealed by our results. These data were obtained using small aspect ratios, suggesting that data for different wormlike micellar solutions and high aspect ratios are still needed.

In general, shear-thinning viscoelastic fluids present three regions of behavior of K/K_N with We (A, B and D), and absence of a plateau region usually found in Boger fluids (region C in Fig. 1). The first region where drag reduction occurs (region B in Fig. 1) is attributed to a less strain-thickening extensional viscosity, while the increase in drag (region D in Fig. 1) is due to the opposite effect. Notwithstanding, a second decrease in drag appears as We increases much further (region E in Fig. 1). This region was explained by Chen and

Rothstein (2004) in terms of saturation of extensional viscosity as micelles approach their finite extensibility limit leading to filament rupture. Finally, despite the onset of extension-thickening in the HASE solutions (see Fig. 2), no evidence of increasing drag correction factor was observed in our results; this behavior may be attributed to the fact that the onset of extension-thickening coincides with that of shear-thinning. The simultaneous action of these opposing mechanisms may offset the drag increase. Clearly, more experiments are needed to fully elucidate this phenomenon.

Conclusions

Results shown in this work demonstrate that the extension-thinning properties of the fluid together with a high value of the characteristic extension rate are the important factors for drag reduction observed in associative polymers. The value of the critical We number where the drag reduction occurs agree with the theoretical value found for extension-thinning (reduction of Trouton ratio) and the experimental conditions for negative wake apparition. Neither evidence of plateau formation at intermediate We numbers, nor drag increase at higher We, were observed. Future investigations in this subject must evaluate the extensional properties of the test liquids to confirm that the onset of extensional thinning is indeed the most relevant factor for the drag reduction to be observed. More experiments for large values of the Weissenberg number ($We > 3$) Are still needed to investigate the nature of drag increase phenomena. These experimental results show that associative polymers can be used as model fluids which have the advantage of being readily accessible, easy to prepare, show stability and exhibit a wide range of fluid properties.

Acknowledgement Support from CONACYT (Consejo Nacional de Ciencia y Tecnología) through the Project 100195 is acknowledged.

References

Arigo M, McKinley G (1997) The effects of viscoelasticity on the transient motion of a sphere in a shear-thinning fluid. J Rheol 41:1–10

Bisgaard C (1983) Velocity fields around spheres and bubbles investigated by laser-doppler anemometry. J Non-Newton Fluid Mech 12:283–293

Chen S, Rothstein J (2004) Flow of a wormlike micelle solution past a falling sphere. J Non-Newton Fluid Mech 116:205–215

Chhabra R (1993) Bubbles, drops and particles in non-Newtonian fluids. CRP Press, New York

Degand E, Walters K (1995) On the motion of a sphere falling through an elastic liquid contained in a tightly-fitting cylindrical container. J Non-Newton Fluid Mech 57: 103–115

Dou H, Phan-Thien N (2004) Criteria of negative wake generation behind a cylinder. Rheol Acta 43:203–213

Elmoumni A, Winter H (2006) Large strain requirements for shear-induced crystallization of isotactic polypropylene. Rheol Acta 45:793–801

Jones W, Price H, Walters K (1994) The motion of a sphere falling under gravity in a constant-viscocity elastic liquid. J Non-Newton Fluid Mech 53:175–196

Mena B, Manero O, Leal L (1987) The influence of rheological properties on the slow flow past spheres. J Non-Newton Fluid Mech 26:247–275

Mendoza-Fuentes A, Montiel R, Zenit R, Manero O (2009) On the flow of associative polymers pasta a sphere: evaluation of negative wake criteria. Phys Fluids 21:033104

Navez V, Walters K (1996) A note on settling in shear-thinning polymer solutions. J Non-Newton Fluid Mech 67: 325–334

Owens R, Phillips T (2002) Computational rheology. Imperial College Press, London

Puig J, Bautista F, Soltero J, Manero O (2007) Nonlinear rheology of giant micelles. In: Giant micelles properties and applications. CRC Press

Sigli D, Coutanceau M (1977) Effect of finite boundaries on the slow laminar isothermal flow of a viscoelastic fluid around a spherical obstacle. J Non-Newton Fluid Mech 2: 1–10

Soto E, Goujon C, Zenit R, Manero O (2007) A study of velocity discontinuity for single air bubbles rising in an associative polymer. Phys Fluids 18:121510

Walters K, Tanner R (2002) The motion of a sphere through an elastic fluid. In: Chhabra R, Kee DD (eds) Transport processes in bubbles, drops and particles, 1st edn. Hemisphere Publishing Corporation, Taylor and Francis Group, New York